Similarity evaluation between neutron multiplication factors and nuclide inventories during nuclear fuel burnup

Hiroki Harada[1,*] and *Go* Chiba[1,**]

[1]Hokkaido University, Faculty of Engineering, Kita 13 Nishi 8, Sapporo, Hokkaido 060-8628, Japan

Abstract. There are several different types of the integral data of nuclear fission systems, and the accuracy of the numerical predictions of them are related with each other via the nuclear data commonly used in the numerical simulations. Thus, it is sometimes possible that measurement data of one type of the integral data are used to improve the prediction accuracy of the different type of the integral data. To quantitatively evaluate such possibility, the similarity of the different types of the integral data is important. In this study, we quantitatively evaluate the similarity between neutron multiplication factors and nuclide inventories during nuclear fuel burnup from the viewpoint of the nuclear data uncertainties using the representativity factors. Using the Burner module of the CBZ reactor physics code system for fuel pin-cell burnup problems, we calculated the sensitivity of the neutron infinite multiplication factors and the inventories of the 17 actinoids at several fuel burnup points. The neutron multiplication factor during the fuel burnup was considered the target parameter for which the prediction accuracy is improved, and the degree of similarity of the nuclide inventory data during burnup to the target was quantitatively evaluated using the representative factor. Subsequently, multiple nuclide inventory data were combined using the concept of the extended bias factor method to create a fictitious parameter, and we investigated how much this fictitious parameter can increase the representativity factor for the target parameter. As a result, the representativity factor for the target parameters could be increased to more than 0.8 using some nuclide inventory data, and up to 0.92 depending on the burnup, even taking into consideration the measurement error.

1 Introduction

Measurement data on reactor core characteristics (integral data) are used for validation of evaluated nuclear data and for data assimilation to improve the accuracy of nuclear data. A typical example of integral data is the effective neutron multiplication factor (or criticality characteristics) of nuclear reactors. Measurement data on the effective neutron multiplication factor of various nuclear reactors is summarized in the ICSBEP Handbook, which is used worldwide. Data related to the nuclear fuel composition (or nuclide inventory) during/after the nuclear fuel burnup are likewise integral data and contribute to the validation and improvement of the accuracy of nuclear data. Recently, a project called EUCLID (Experiments Underpinned by Computational Learning for Improvements in nuclear Data) was started at Los Alamos National Laboratory[1, 2]. This project focuses on integral data other than effective neutron multiplication factors and actively uses them to verify and improve the accuracy of nuclear data. Nuclide inventory data are not explicitly referred in the paper of EUCLID, but these are also the integral data and are expected to have characteristics not found in other integral data. Therefore, it would be essential data for validating and improving the accuracy of nuclear data. However, there have been no quantitative examples demonstrating its features and uniqueness. For this reason, in this study, we examine the usefulness of nuclide inventory data.

The sensitivity coefficient of the integral data with respect to the nuclear data is useful, and sensitvities of parameters related to the fuel burnup, *burnup sensitivities*, can be calculated by the depletion perturbation theory[3, 4].The reactor physics code system CBZ, which is under development at Hokkaido University, would be the only code having the capability to calculate the burnup sensitivity of complex systems such as LWR (light water reactor) fuel assemblies[5]. By using CBZ, it is possible to quantitatively evaluate the characteristics of the sensitivity of the nuclide inventory data and the degree of its similarity to the neutron multiplication factor data.

2 Theory and procedure

In the present work, we evaluated the degree of similarity of the nuclide inventory data to the target parameter, the neutron infinite multiplication factor k_∞, of the fuel pin cell during burnup. More specifically, we calculated the sensitivity of k_∞ and the inventories of the 17 actinoids at concerning fuel burnup points using the Burner module of CBZ. Based on the calculated sensitivities, representativity factors (RFs) [6–9] between the target parameters and

*e-mail: hirokih0114bbpcf8@eis.hokudai.ac.jp
**e-mail: go_chiba@eng.hokudai.ac.jp

the nuclide inventory data were also calculated in order to evaluate the similarity. Then, we examined how much the RF could be increased by using multiple nuclide inventory data. The concept of the extended bias factor method[10] was used to combine multiple nuclide inventory data.

2.1 Representativity factor

Let $\mathbf{S}_i$ and $\mathbf{S}_j$ be the sensitivity vectors of the target parameter i and the mockup parameter j, and let $\mathbf{V}$ be the covariance matrix of the nuclear data. The RF r is defined as follows:

$$r = \frac{\mathbf{S}_i^T \mathbf{V} \mathbf{S}_j}{\sqrt{\mathbf{S}_i^T \mathbf{V} \mathbf{S}_i} \sqrt{\mathbf{S}_j^T \mathbf{V} \mathbf{S}_j}}. \tag{1}$$

The RF is the correlation between the two integral data including the nuclear data-induced uncertainties. The closer this absolute value is to unity, the more similar the data are in terms of nuclear data uncertainty. The degree of the similarity is important when the information on the mockup parameter is used to improve the prediction accuracy of the target parameter by the bias factor method[11]. Regarding the uncertainty (variance) of the prediction of the target parameters, let ΔR_0^2 be the uncertainty evaluated without the bias factor method and ΔR_1^2 with the bias factor method. There is the following relationship between them[6]:

$$\Delta R_1^2 = \Delta R_0^2 \left(1 - r^2\right). \tag{2}$$

In other words, the RF also represents how much the uncertainty of the target parameter is reduced by the bias factor method using information from the mockup parameter.

2.2 Extended bias factor method

While the classical bias factor method uses data from a single mockup parameter, the use of multiple parameters can further reduce uncertainty in target parameter predictions. One such method is the extended bias factor method[10]. In the bias correction, it is important to prepare mockup parameter whose sensitivity is similar to the sensitivity of the target parameter. The extended bias factor method attempts to reproduce the sensitivity of the target parameter by superimposing the sensitivities of multiple mockup parameters. The extended bias factor method deals with errors due to nuclear data, errors due to calculation methods, and measurement errors, but for the sake of simplicity, we focus only on errors due to nuclear data.

Let p_i denote multiple mockup parameters, and define the fictitious parameter p as

$$p = \prod_i p_i^{a_i}. \tag{3}$$

The partial differentiation of p with respect to p_i was performed as

$$\frac{\partial p}{\partial p_i} = a_i p_i^{a_i - 1} \prod_{j \neq i} p_j^{a_j} = \frac{a_i}{p_i} p_i^{a_i} \prod_{j \neq i} p_j^{a_j} = \frac{a_i}{p_i} p, \tag{4}$$

and the following equation is obtained:

$$\frac{\partial p}{\partial p_i} \cdot \frac{p_i}{p} = a_i. \tag{5}$$

Thus, the sensitivity of p to nuclear data σ, S_σ^p, can be represented as

$$S_\sigma^p = \frac{\partial p}{\partial \sigma} \cdot \frac{\sigma}{p} = \sum_i \frac{\partial p}{\partial p_i} \cdot \frac{p_i}{p} \cdot \frac{\partial p_i}{\partial \sigma} \cdot \frac{\sigma}{p_i} = \sum_i a_i S_\sigma^{p_i}. \tag{6}$$

This equation means that the sensitivity of the fictitious parameter p is expressed by the linear combination of the sensitivities of multiple mockup parameters. Next, let us evaluate the uncertainty of the predictions when using the bias factor for the fictitious parameter p. As mentioned above, we ignore uncertainties due to other than nuclear data for the sake of simplicity. The variance V_p for the calculated value of parameter p can be written as

$$\begin{aligned} V_p &= \sum_i \sum_j \left(\frac{\partial p}{\partial p_i} \cdot \frac{p_i}{p}\right)\left(\frac{\partial p}{\partial p_j} \cdot \frac{p_j}{p}\right) \mathrm{cov}\left(p_i, p_j\right) \\ &= \sum_i \sum_j a_i a_j \,\mathrm{cov}\left(p_i, p_j\right) = \sum_i \sum_j a_i a_j \mathbf{S}_i^T \mathbf{V} \mathbf{S}_j. \end{aligned} \tag{7}$$

Let p_R be the target parameter to be predicted. The variance for the calculated value of p_R can be expressed using the sensitivity vector of the target parameter, $\mathbf{S}_R$, as

$$V_{p_R} = \mathbf{S}_R^T \mathbf{V} \mathbf{S}_R. \tag{8}$$

Since the covariance of the calculated values of p and p_R is represented as

$$\mathrm{cov}\left(p, p_R\right) = \sum_i a_i \mathbf{S}_i^T \mathbf{V} \mathbf{S}_R, \tag{9}$$

the uncertainty of $\tilde{p}_R$ which is the predicted value of p_R using the bias factor method, $V_{\tilde{p}_R}$, is represented as

$$\begin{aligned} V_{\tilde{p}_R} &= V_p + V_{p_R} - 2\,\mathrm{cov}\left(p, p_R\right) \\ &= \sum_i \sum_j a_i a_j \mathbf{S}_i^T \mathbf{V} \mathbf{S}_j + \mathbf{S}_R^T \mathbf{V} \mathbf{S}_R - 2 \sum_i a_i \mathbf{S}_i^T \mathbf{V} \mathbf{S}_R \\ &= \left(\mathbf{S}_R - \sum_i a_i \mathbf{S}_i\right)^T \mathbf{V} \left(\mathbf{S}_R - \sum_i a_i \mathbf{S}_i\right). \end{aligned} \tag{10}$$

The exponents a_i in the fictitious parameter p are determined from the condition $\frac{\partial V_{\tilde{p}_R}}{\partial a_i} = 0$, which minimizes $V_{\tilde{p}_R}$:

$$\sum_j a_j \mathbf{S}_i^T \mathbf{V} \mathbf{S}_j - \mathbf{S}_i^T \mathbf{V} \mathbf{S}_R = 0, \quad (i = 1, \ldots, N), \tag{11}$$

where N is the number of mockup parameters. When we define $\mathbf{A} = (a_1, a_2, \ldots, a_N)^T$ and $\mathbf{S} = (\mathbf{S}_1 \quad \mathbf{S}_2 \ldots \mathbf{S}_N)$, then the above equation can be rewritten as follows:

$$\mathbf{S}^T \mathbf{V} \mathbf{S} \mathbf{A} = \mathbf{S}^T \mathbf{V} \mathbf{S}_R. \tag{12}$$

Thus, $\mathbf{A}$ is calculated as

$$\mathbf{A} = \left(\mathbf{S}^T \mathbf{V} \mathbf{S}\right)^{-1} \left(\mathbf{S}^T \mathbf{V} \mathbf{S}_R\right). \tag{13}$$

If the matrix $\mathbf{S}^T \mathbf{V} \mathbf{S}$ is singular, the pseudo-inverse matrix can be used instead of the normal inverse matrix.

3 Target system and burnup calculation conditions

The target system of the present study is a PWR-UO2 pin-cell with a U-235 enrichment of 4.1%. Line power density is set at 179 W/cm and fuel burnup up to 40 GWd/t is concerned. As nuclear data, JENDL-4.0 was used for neutron reaction cross sections, JENDL/FPD-2011 for decay data, and JENDL/FPY-2011 for fission yield data. For the burnup calculations, a simplified burnup (nuclide transmutation) chain consisting of 21 actinides and 138 fission products was used. Under the above burnup conditions, the sensitivity of k_∞ was calculated from 0 to 40 GWd/t in 5 GWd/t steps. For the same pin-cell, the sensitivity of the nuclide inventory was calculated from 5 to 40 GWd/t in 5 GWd/t steps. The mockup nuclide inventory data were for 17 nuclides excluding U-238 and the short-lived nuclides U-237, Np-239, and Am-242 from the heavy nuclides included in the chain used. Covariance data for nuclear data are required for the calculation of RFs. In this study, only covariance data for the reaction cross section of actinides were considered, and the JENDL-4.0 evaluation data were used.

4 Results

4.1 Maximum representativity factor calculation

The nuclear data-induced uncertainty of k_∞ of the target system is shown in **Figure 1**. The uncertainty at the beginning of the burnup is largely due to the capture cross section of U-238, and at the end it is largely due to the capture cross section of Pu-241. Additionally, the nuclear data-induced uncertainty of 17 nuclides inventory data for several burnup points is shown in **Figure 2**.

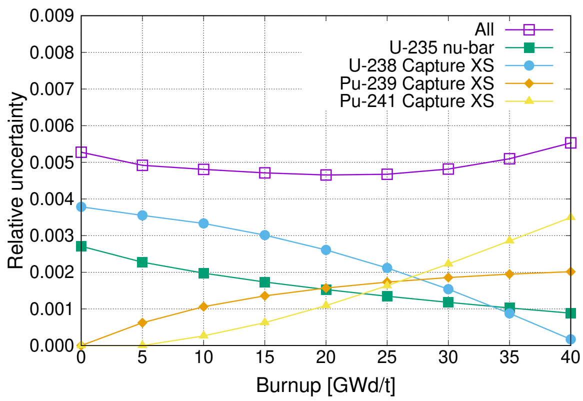

Figure 1. Total and component-wise nuclear data-induced uncertainty of k_∞

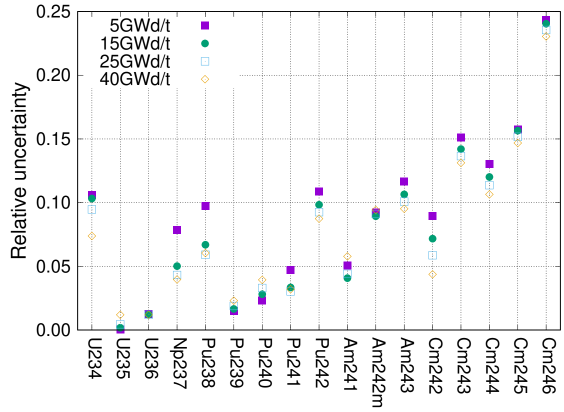

Figure 2. The Nuclear data-induced uncertainty of inventory data

The target parameters were set as k_∞ at 9 burnup points (0-40 GWd/t). We calculated RFs of all nuclide inventory data for all burnup points (5-40 GWd/t) for each target k_∞. The largest calculated RFs are shown in **Figure 3** and the corresponding mockup data are shown in **Table 1** as Case 1. The RF was about 0.75 at the beginning and end of the burnup, and about 0.55 at the middle. The mockup data yielding the largest RF was Pu-239 at the beginning and switched to Pu-242 as the burnup proceeds. Plutonium-239 and -242 are produced by the neutron capture reactions of U-238 and Pu-241, respectively, and these reaction cross sections are main contributors to the k_∞ uncertainties as shown in Figure 1.

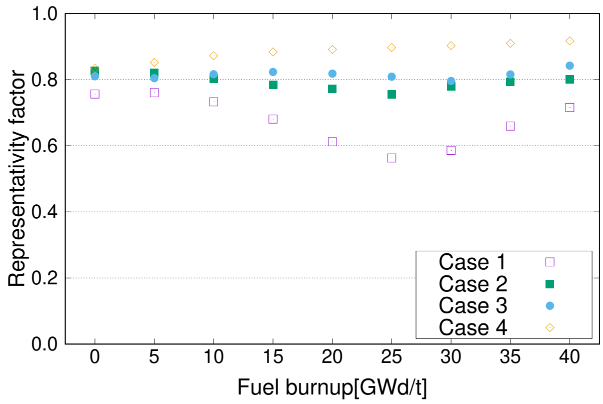

Figure 3. Maximum RFs of nuclide inventory data

https://doi.org/10.1051/epjconf/202328100021

Table 1. Mockup parameters and their combinations with which the maximum RFs are obtained

Target (GWd/t)	Case 1	Case 2		Case 3
0	Pu-239 5GWd/t	U-236 5GWd/t	Pu-239 5GWd/t	U-235
5	Pu-239 5GWd/t	U-235 5GWd/t	Pu-239 5GWd/t	U-235
10	Pu-239 5GWd/t	U-235 5GWd/t	Pu-239 40GWd/t	Pu-240
15	Pu-239 5GWd/t	Pu-240 15GWd/t	Pu-241 10GWd/t	Pu-240
20	Pu-239 40GWd/t	Pu-240 20GWd/t	Pu-241 5GWd/t	Pu-241
25	Pu-240 5GWd/t	Pu-240 5GWd/t	Pu-242 10GWd/t	Pu-241
30	Pu-242 10GWd/t	Pu-240 5GWd/t	Pu-242 15GWd/t	Pu-241
35	Pu-242 30GWd/t	Pu-240 5GWd/t	Pu-242 30GWd/t	Pu-242
40	Pu-242 40GWd/t	Pu-240 10GWd/t	Pu-242 35GWd/t	Pu-242

Next, in order to increase RF, a fictitious parameter was created using multiple nuclide inventory data by the extended bias factor method, and RFs for the targets were calculated. We considered three cases to combine multiple data: Cases 2, 3, and 4. In Case 2, we created fictitious parameters by combining two nuclide inventory data. In this case, the sensitivities of the same nuclide at different burnup points were not combined. In Case 3, we combined nuclide inventory data of unique nuclide at 8 burnup points from 5 to 40 GWd/t, and in Case 4 all the treated nuclide inventory data were combined.

The results are shown in Figure 3. For Cases 2 and 3, the maximum RFs among possible combinations are presented. The combinations yielding maximum RFs for Cases 2 and 3 are shown in Table 1. It is clear that the combination of multiple data can reduce the uncertainty of the target prediction.

In all of Cases 2, 3, and 4, the RF could be increased to 0.75 or higher by combining multiple data. In Case 2, the combination of data included Pu-239 at the beginning of the burnup and Pu-242 at the middle and end. In Case 3, it was found that, depending on the burnup of the target, RF could be increased to about 0.85 even with data for only one nuclide. Also here, it was found that the mockup inventory data yielding the maximum RF changed from U-235 to Pu-242 as the fuel burnup proceeds. In Case 4, since all data were utilized, the RF is theoretically increased to the maximum among all the cases. It can be seen that there is a limit to increasing the RF at the beginning of the burnup. This is due to the relatively large contribution of the number of neutrons produced per fission $\bar{\nu}$ of U-235. Since $\bar{\nu}$ has no significant effect on the nuclide inventory, it is difficult to reduce the uncertainty due to $\bar{\nu}$ only with the nuclide inventory data.

4.2 Identification of the important mockup parameters in the fictitious mockup parameters

Next, we attempt to identify the important mockup parameters in Case 4. First, we focus on the weights of the mockup parameters in the fictitious parameters determined by the extended bias factor method. The weights of each mockup parameter when targeting k_∞ at 40 GWd/t are shown in **Figure 4**. The range of the weights taken is quite wide and expands from -200 to 150. In this case, it is possible for nuclides having negligibly small sensitivities to have large weights relative to its importance. Therefore, by using weights alone, we cannot identify important mockup parameters. As another approach, weight of the mockup parameters was changed to zero individually and the amount of reduction in RF was quantified. Only the weights of the individual mockup data were reset to zero, and the other mockup data weights were not changed. It means that we did not perform the extended bias factor calculation where one mockup data was removed. The results are shown in **Figure 5**. There were some cases where the reduction in RF exceeded 0.9 (i.e., the RF became negative) when the weight of only one mockup parameter was set to zero.

We investigate this large reduction in RF. When k_∞ at 40 GWd/t is concerned, the main source of the uncertainty due to nuclear data is the capture cross section of Pu-241. The sensitivity of the target to the Pu-241 capture cross section and that reproduced using the extended bias factor method are shown in **Figure 6**. We can confirm that the sensitivity of the target is well reproduced. The fictitious parameter was created by linear combination of the sensitivities of the 17 nuclides × 8 burnup points as previously described. Among the mockup parameters, the sensitivities of the Cm-245 number density at 5 GWd/t and the Np-237 number density at 35 GWd/t to the Pu-241 capture cross section multiplied by their weights are shown in **Figure 7**. It can be found that the target sensitivity is reproduced by the cancellation of the large positive and negative sensitivities.

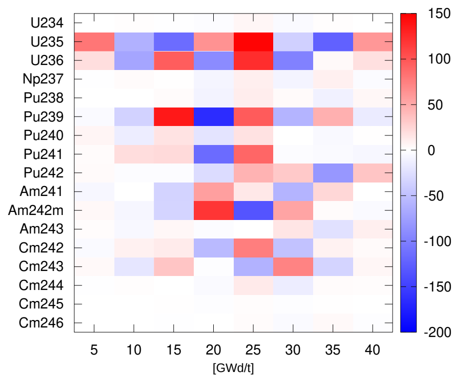

Figure 4. Weights of individual mockup parameters in the fictitious mockup parameters for k_∞ at 40 GWd/t (Case 4)

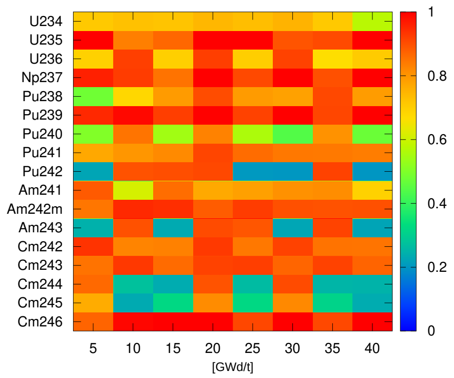

Figure 5. Reduction of RFs when setting individual weights zero (target: k_∞ at 40 GWd/t, Case 4)

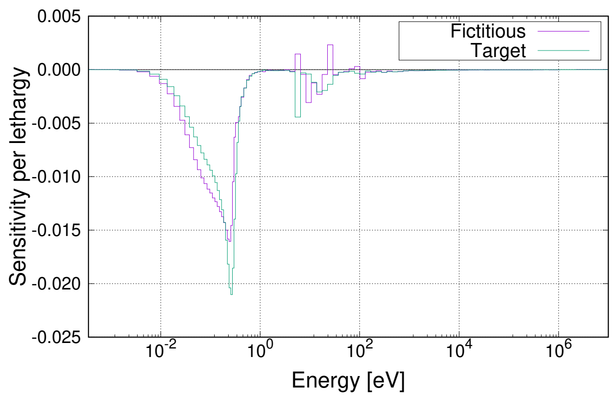

Figure 6. Sensitivities of target and fictitious parameters to Pu-241 capture cross section in Case 4

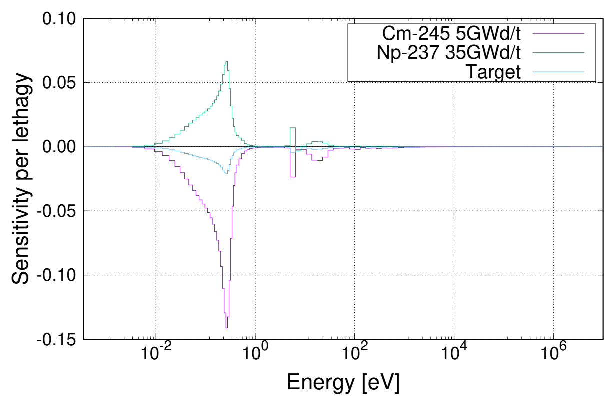

Figure 7. Decomposed sensitivities of fictitious parameters to Pu-241 capture cross section in Case 4

The above calculations use the extended bias factor method that deals only with errors due to nuclear data for simplicity. In this case, if measurement error is taken into consideration in some way, the uncertainty of the fictitious parameters becomes very large when large weights are given to individual mockup parameters. This makes the prediction error by the extended bias factor method worse significantly. Therefore, we reexamined the importance of mockup parameters by taking into consideration the measurement error of the mockup parameters. In the reference[11], RF that takes into consideration the measurement error of the mockup parameters is defined as follows:

$$\hat{r} = r \cdot \frac{\sqrt{V_c}}{\sqrt{V_c} + \sqrt{V_e}}, \tag{14}$$

where V_c represents the uncertainty (variance) due to nuclear data and V_e is the measurement error in the mockup parameters. Using this equation, the variance of the predictions by the bias factor method is modified as follows[11]:

$$\Delta R_1^2 = \Delta R_0^2 \left(1 - \hat{r}^2\right) = \Delta R_0^2 \left(1 - \frac{r^2}{1 + \frac{V_e}{V_c}}\right). \tag{15}$$

Thus, when the measurement error of the mockup parameters (V_e) is large, it is difficult to reduce the variance of the predictions even if r is close to unity. The weights of the extended bias factor method are determined by the following equation when measurement error is taken into consideration:

$$\mathbf{A} = \left(\mathbf{S}^T\mathbf{V}\mathbf{S} + \mathbf{V}_e\right)^{-1}\left(\mathbf{S}^T\mathbf{V}\mathbf{S}_R\right). \tag{16}$$

In the present work, the measurement error was assumed 0.5 % for all nuclide inventory data, and RF was recalculated in the same way as in Case 4. The results are shown in **Figure 8** as Case 4-2. The values of RF did not change significantly after the measurement error consideration. We attempted to identify the important mockup parameters from the same two perspectives as before. The results for k_∞ at 40 GWd/t are shown in **Figures 9** and **10**. Mockup parameters with extremely large weights do not appear when measurement errors are taken into consideration, and it is confirmed that many nuclides contribute universally to the reproduction of the target sensitivity. Compared to Case 4, the RF is no longer significantly reduced by setting only one weight to zero. The sensitivity of the target to the Pu-241 capture cross section and the sensitivity reproduced using the extended bias factor method to consider measurement error are shown in **Figure 11**. The sensitivity was found to be well reproduced in Case 4-2. The sensitivities of the Cm-244 number density at 10 and 40 GWd/t and the Am-243 number density at 5 GWd/t to the Pu-241 capture cross section multiplied by their weights are shown in **Figure 12**. Even in Case 4-2, cancellation of positive and negative sensitivities occurred. However, unlike Case 4, the norm of decomposed sensitivity vectors of the fictitious mockup parameter is no longer larger than the norm of sensitivity vector of the target.

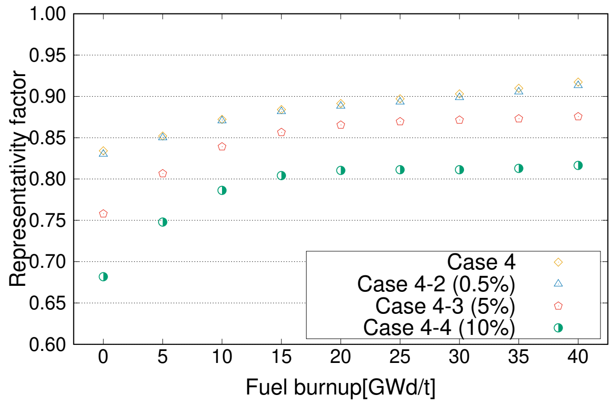

Figure 8. Maximum RFs of nuclide inventory data taking into consideration measurement error

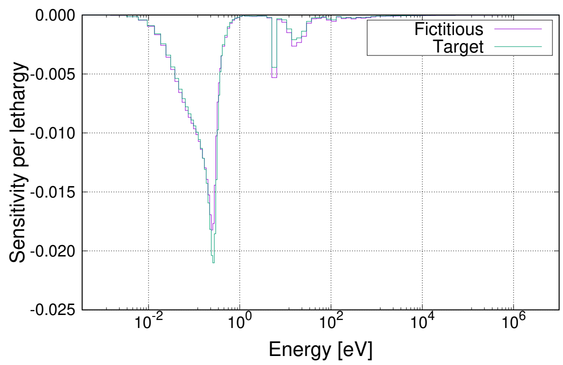

Figure 11. Sensitivity of target and fictitious parameter (Pu-241 capture,Case4-2)

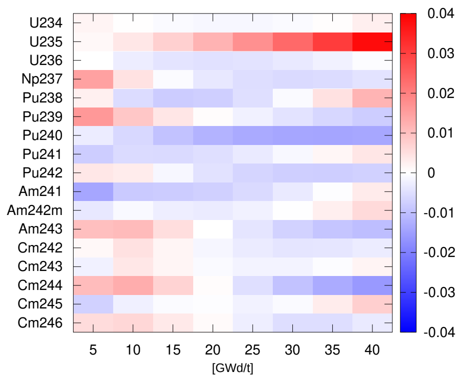

Figure 9. Weights of individual mockup parameters in the fictitious mockup parameters for k_∞ at 40 GWd/t (Case 4-2)

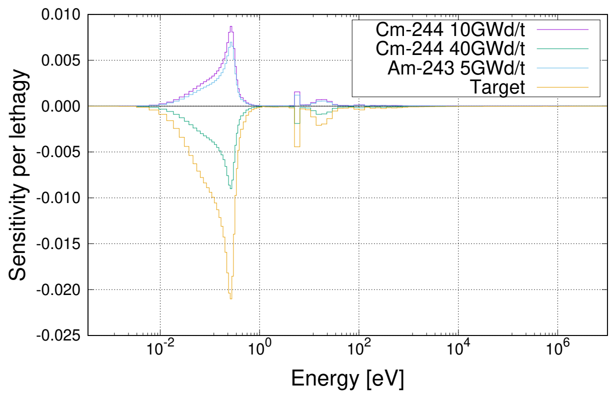

Figure 12. Decomposed sensitivities of fictitious parameters to Pu-241 capture cross section in Case4-2

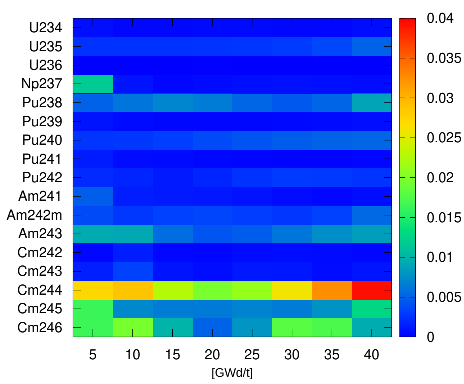

Figure 10. Reduction of the RFs when making individual weights zero (target: k_∞ at 40 GWd/t, Case 4-2)

In addition, we made the same calculations assuming a measurement error of 5 % or 10 % for all nuclide inventory data. The results are shown in **Figure 8** as Cases 4-3 and 4-4. In Case 4-3 the RF is about 0.75 at the beginning of the burnup and approached 0.88 as the burnup proceeds. In Case 4-4 the RF is about 0.68 at the beginning of the burnup and approached 0.82 as the burnup proceeds. We also attempted to identify important mockup parameters. The results for k_∞ at 40 GWd/t in Case 4-3 are shown in **Figures 13** and **14**. When the measurement error is set to 5%, the range of weights taken is smaller compared to 0.5%. The reduction of the RFs when making individual weights zero is also smaller. From the above, mockup parameters with extremely large weights do not appear when measurement errors are taken into consideration, and it is confirmed that many nuclides contribute universally to the reproduction of the target sensitivity. Compared to Case 4, the RF is no longer significantly reduced by setting only one weight to zero.

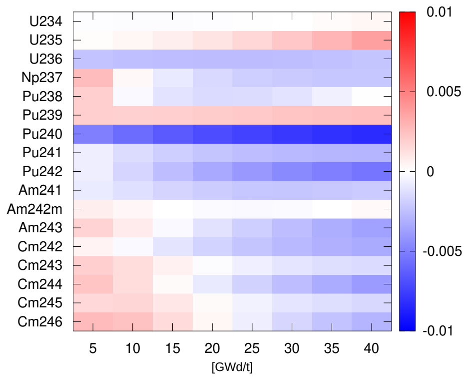

Figure 13. Weights of individual mockup parameters in the fictitious mockup parameters for k_∞ at 40 GWd/t (Case 4-3)

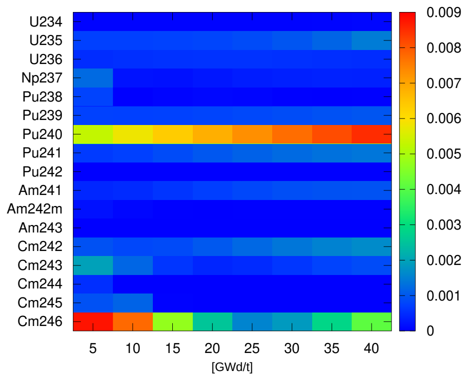

Figure 14. Reduction of the RFs when making individual weights zero (target: k_∞ at 40 GWd/t, Case 4-3)

5 Conclusion

The relationship between burnup quantity and criticality characteristics was quantified using RFs. The RFs for neutron infinite multiplication factor and nuclide inventory data were about 0.75 at the beginning and end of the burnup, and about 0.6 at the middle. We confirmed that the extended bias factor method can be used to create fictitious parameters which increase the RF with the target. The extended bias factor method here dealt only with uncertainties due to nuclear data. By combining multiple nuclide inventory data, we were able to increase RF to neutron infinite multiplication factor to about 0.92. By checking fictitious parameter combinations, it was found that Pu-239 and Pu-242 play important roles in reproducing the sensitivities of the target at the beginning and middle/end of the burnup.

When fictitious parameters were created using the extended bias factor method with a large number of mockup parameters, the weights for the mockup parameters became extremely large. We have only dealt with uncertainties due to nuclear data, but if the mockup parameters have measurement errors, the uncertainty of the fictitious parameter would become extremely large when large weights are given to individual mockup parameters. Therefore, the extended bias factor method was applied again assuming a measurement error of 0.5% or 5% for the mockup data. The weights of the individual mockup parameters were not extremely large, and we were able to create fictitious parameters in which many nuclides contributed universally. The RF with the target was about 0.8, even when considering a 10% measurement error in the inventory data. From the above, it can be said that burnup quantity data are useful for criticality characteristics data.

References

[1] M. Herman, et al., "Infrastructure for the new paradigm of nuclear reaction evaluation," Ann. Nucl. Energy, 163, 108494 (2021).

[2] J. Hutchinson, et al., "Investigation of delayed neutron sensitivities for several ICSBEP benchmarks using MCNP," Trans. Am. Nucl. Soc., 125, p.620 (2021).

[3] A. Gandini, "A method of correlation of burnup measurements for physics prediction of fast power-reactor life," Nucl. Sci. Eng., 38, p.1 (1969).

[4] M. L. Williams, "Development of depletion perturbation theory for coupled neutron/nuclide field," Nucl. Sci. Eng., 70, p.20 (1979).

[5] G.Chiba, H.Harada, "Validation of LWR fuel depletion calculation module of reactor physics code system CBZ," J. Nucl. Sci. Technol., (accepted).

[6] G. Palmiotti, M. Salvatores, "Use of integral experiments in the assessment of large liquid-metal fast breeder reactor basic design parameters," Nucl. Sci. Eng., 87, p.333 (1984).

[7] M. Plaschy, et al., "Importance of the MUSE experiments for emerging ADS concepts from the nuclear data viewpoint," Ann. Nucl. Energy, 32, p.843 (2005).

[8] P.T. Krishna Kumar, et al., "Maximization of representativity factors for experimental planning of cross-section measurements: an information theoretic approach," Ann. Nucl. Energy, 35, p.2243 (2008).

[9] J.F. Lebrat, et al., "The use of representativity theory in the depletion calculations of SFR blankets," Ann. Nucl. Energy, 101, p.429 (2017).

[10] T. Kugo, T. Mori, T. Takeda, "Theoretical study on new bias factor methods to effectively use critical experiments for improvement of prediction accuracy of neutronics characteristics", J. Nucl. Sci. Technol., 44, p.1509 (2007).

[11] A. Gandini, "Uncertainty analysis and experimental data transposition methods based on perturbation theory," in Y. Ronen (Ed.) "Uncertainty Analysis", CRC press, (1988)